

Grain size effect on cyclic oxidation of (TiB₂+TiC)/Ni₃Al composites

CAO Guo-jian¹, XU Hong-yu², ZHENG Zhen-zhu², GENG Lin², Naka Masaaki³

1. School of Materials Science and Engineering, Harbin University of Science and Technology, Harbin 150040, China;

2. School of Materials Science and Engineering, Harbin Institute of Technology, Harbin 150001, China;

3. Joining and Welding Research Institute, Osaka University, Ibaraki, Osaka 567-0047, Japan

Received 18 August 2011; accepted 28 October 2011

Abstract: (TiB₂+TiC)/Ni₃Al composites were prepared by mechanical alloying of elemental powders and subsequently spark plasma sintering. Microstructure of (TiB₂+TiC)/Ni₃Al composite sintered at 950 °C was finer than that of composite sintered at 1050 °C. The influence of grain size on cyclic oxidation behavior was investigated. Cyclic oxidation results showed that the composite sintered at 950 °C had smaller mass gains than the composite sintered at 1050 °C. XRD and EDS results indicate that finer grain size is beneficial for increasing the oxidation resistance by improving the formation of a continuous TiO₂ outer layer and a continuous Al₂O₃ inner layer on the surface of the composites sintered at 950 °C.

Key words: nickel aluminides; composites; grain refinement; oxidation; mechanical alloying

1 Introduction

Intermetallic compound Ni₃Al is of a great interest for its attractive applications in aerospace and power industries as a high-temperature structural material due to its low density, high strength and good oxidation resistance at elevated temperatures [1,2]. However, the practical use of Ni₃Al is still severely restricted by its low-temperature brittleness and poor high-temperature creep resistance. One approach to enhance the high-temperature strength and the high-temperature creep resistance is to reinforce the brittle intermetallic matrix with appropriate volume fraction of ceramic phases, which may provide a good combination of high-temperature strength, creep resistance, environmental stability with adequate ambient temperature ductility [3,4].

For application at high temperature, it is essential that mechanical properties of Ni₃Al were improved without lowering its high-temperature oxidation resistance. Ni₃Al exhibits an excellent oxidation resistance because of its capability of forming a continuous Al₂O₃ layer below an outer layer of NiO and an intermediate layer of NiAl₂O₄ at high temperatures [5]. However, the addition of ceramic particles like TiB₂ and (or) TiC may reduce

the oxidation resistance by the formation of discontinuous oxide layers. Some researchers [6–8] reported that Ni₃Al compound with fine microstructure obtained good anti-oxidation ability since increased grain boundaries (GBs) can promote the selective oxidation of Al to form continuous oxide layer in cyclic oxidation of Ni₃Al. It is reasonable to deduce that grain refinement may be a possible way to optimize the oxidation performance of (TiB₂+TiC)/Ni₃Al composites. The effect of grain size on oxidation resistance of Ni₃Al matrix composites has not been researched quit well.

To achieve fine microstructure, spark plasma sintering (SPS) is an effective technique, which fabricates materials by charging a high pulsed electric current directly through powders in a graphite die under externally applied pressure [9–11].

In this study, the microstructure and cyclic oxidation of (TiB₂+TiC)/Ni₃Al composites were examined. Effect of grain size on cyclic oxidation performance was investigated.

2 Material and methods

In this work, 20%(TiB₂+TiC)/Ni₃Al composites (volume fraction), in which the volume ratio of TiB₂ to TiC was 1:1, were prepared by using mechanical alloying

method. Starting powders used in this study were elemental Ni (99.9% purity, 3 μm), Al (99.9% purity, 3 μm), Ti (99.9% purity, 10 μm), B (99.7% purity, 1 μm) and C (99.7% purity, 1 μm) powders. The elemental powders were ball milled in a vibration ball milling machine equipped with water-cooled chambers for 30 h prior to sintering by SPS. The ball-to-powder mass ratio was 10:1. Ball milling was performed under an Ar gas atmosphere to prevent the oxidation of the powders during the process. After ball milling, the powders were sintered in a DR. SINTER type SPS-1050 apparatus (Sumitomo Coal Mining Co. Ltd.). The powders were heated in a vacuum of 10 Pa to 950 $^{\circ}\text{C}$ (or 1050 $^{\circ}\text{C}$) at a heating rate of 150 $^{\circ}\text{C}/\text{min}$ for a holding time of 10 min. During SPS process, a uniaxial pressure of 65 MPa was applied to punches. And then, after a cooling process with a rate of 100–40 $^{\circ}\text{C}/\text{min}$, (TiB₂+TiC)/Ni₃Al composites were achieved.

Samples with dimensions of 10 mm \times 10 mm \times 1 mm were cut from the composites by an electro-discharge machine. All samples were metallographically polished, and then cleaned ultrasonically in acetone, and dried in air. The mass and the size of the samples were measured carefully before oxidation exposure. Cyclic oxidation experiments were conducted at 900 $^{\circ}\text{C}$ in air. The samples were withdrawn from furnace every 2 h and cooled to room temperature, weighed before being put back into the furnace. The mass change during exposure was measured by an electron balance with a sensitivity of ± 0.01 mg.

Microstructure of the composites was observed by scanning electron microscopy (SEM) and transmission electron microscopy (TEM). Phases in sintered composites were identified by X-ray diffraction (XRD). The oxidation scales formed at 900 $^{\circ}\text{C}$ for 2 h and 50 h were examined by α -2 θ mode XRD with a 3 $^{\circ}$ incident angle (α). Cross-section of the oxidation samples was observed by SEM equipped with an energy-dispersive spectroscope (EDS). Before SEM observation, the composites before and after oxidation were metallographically polished without erosion.

For convenient, the 20%(TiB₂+TiC)/Ni₃Al composites fabricated at 950 $^{\circ}\text{C}$ and 1050 $^{\circ}\text{C}$ were signed as IC-950 and IC-1050, respectively. The composites synthesized at 950 $^{\circ}\text{C}$ and 1050 $^{\circ}\text{C}$ exhibited relative density of 99.1% and 99.8%, respectively, as measured by the Archimede's method.

3 Results and discussion

3.1 Microstructure of composites

XRD patterns of the 20%(TiB₂+TiC)/Ni₃Al composites fabricated by mechanical alloying and SPS at 950 $^{\circ}\text{C}$ and 1050 $^{\circ}\text{C}$ are shown in Figs. 1(a) and (b),

respectively. Both composites consist of Ni₃Al, TiB₂ and TiC. No other phases are found in the XRD patterns.

Hardness of the composites was tested by using Vickers-hardness. The hardness values of IC-950 and IC-1050 were 8.5 GPa and 9.1 GPa, respectively. These values are much higher compared with coarse Ni₃Al compound, which was reported by PAUL to be 3 GPa [12], meaning that ceramic addition and grain refinement can effectively improve the hardness of the composites.

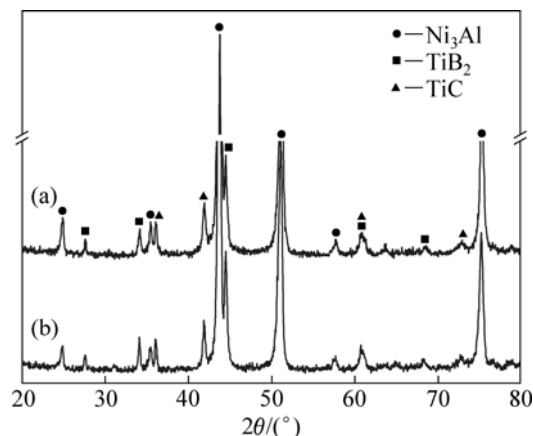


Fig. 1 XRD patterns of (TiB₂+TiC)/Ni₃Al composites sintered at 950 $^{\circ}\text{C}$ (a) and 1050 $^{\circ}\text{C}$ (b)

Grain sizes of phases in the composites could be estimated by Scherrer equation according to peak broadening. However, the estimated grain sizes of different composites are in the same magnitude, which is not coincident with Fig. 2. The reason for this is that the peak broadening is not only due to the reduction of the particle size but also due to the significant residual strain.

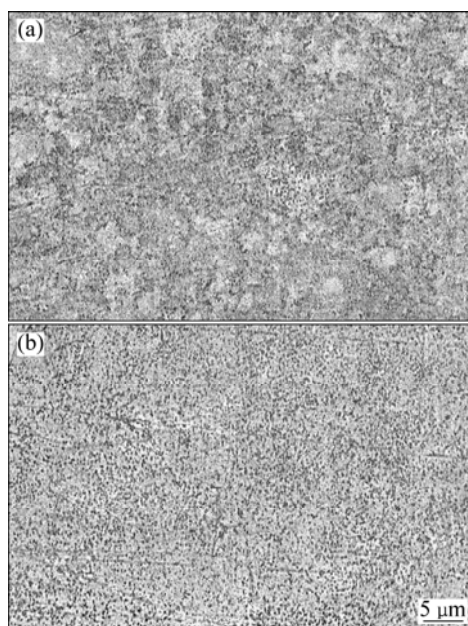


Fig. 2 Backscattered electron images of (TiB₂+TiC)/Ni₃Al composites sintered at 950 $^{\circ}\text{C}$ (a) and 1050 $^{\circ}\text{C}$ (b)

Backscattered electron (BSE) images of both sintered composites are shown in Fig. 2. Gray areas are ceramic phases (TiB_2 or TiC) and bright area is Ni_3Al phase. It can be seen that although both composites are nearly uniform, the microstructures of IC-1050 is more even than those of IC-950. The microstructure in IC-950 is much finer than that in IC-1050. This can be approved by TEM observation shown in Fig. 3. The spacing between ceramic particles in IC-950 is greatly reduced compared with IC-1050.

Bright field TEM images of both composites shown in Fig. 3 show that grains in both composites are essentially equiaxed. The grain sizes of Ni_3Al and ceramic particles are in the same magnitude in each composite. The average grain sizes in IC-950 and IC-1050 are ~ 40 nm and ~ 300 nm, respectively. These indicate that lower sintering temperature can effectively stunt grain growth in the composites.

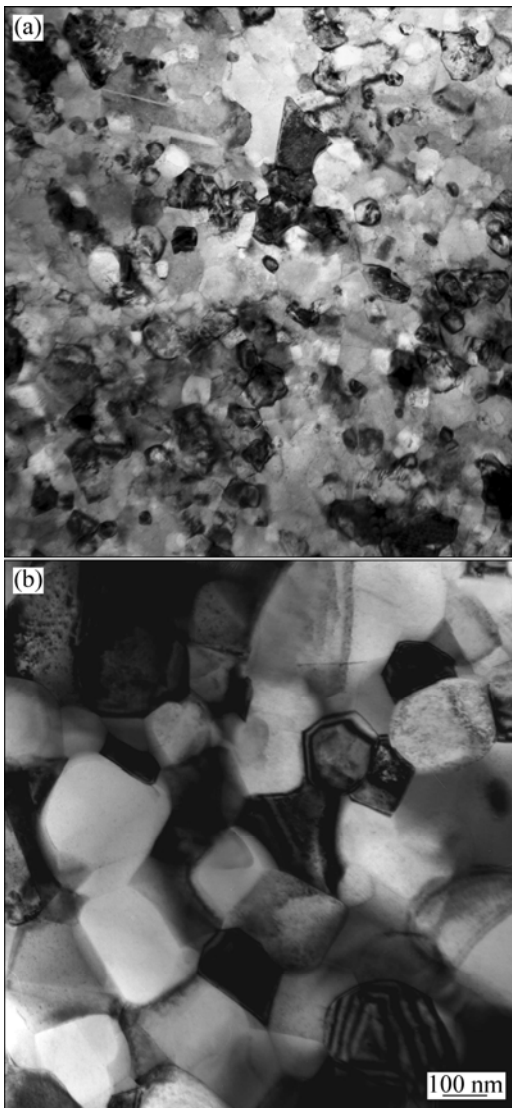


Fig. 3 TEM bright-field images of $(\text{TiB}_2+\text{TiC})/\text{Ni}_3\text{Al}$ composites sintered at 950 °C (a) and 1050 °C (b)

3.2 Cyclic oxidation of composites

Mass changes of both composites cyclically oxidized at 900 °C for 50 h are shown in Fig. 4. Compared with IC-1050, IC-950 shows considerable improvement in oxidation resistance. The excellent oxidation resistance for IC-950 is due to the formation of a dense TiO_2 scale in a short time, and the formation of double continuous oxide layers after longer oxidation. These can be testified by XRD and SEM observations on the oxide scales formed on both composites.

Surface morphologies of the oxide scales formed on both composites after 2 h oxidation in air at 900 °C are shown in Fig. 5. The oxide scales formed on IC-950 are much finer and denser than those formed on IC-1050. Pores are obviously seen in the oxide scales formed on

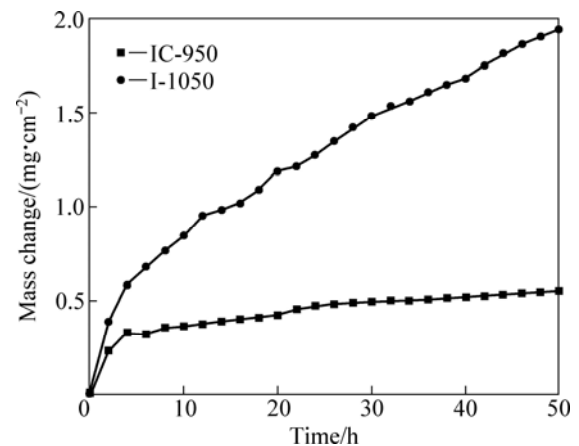


Fig. 4 Cyclic mass change curves of $(\text{TiB}_2+\text{TiC})/\text{Ni}_3\text{Al}$ composites oxidized in air at 900 °C

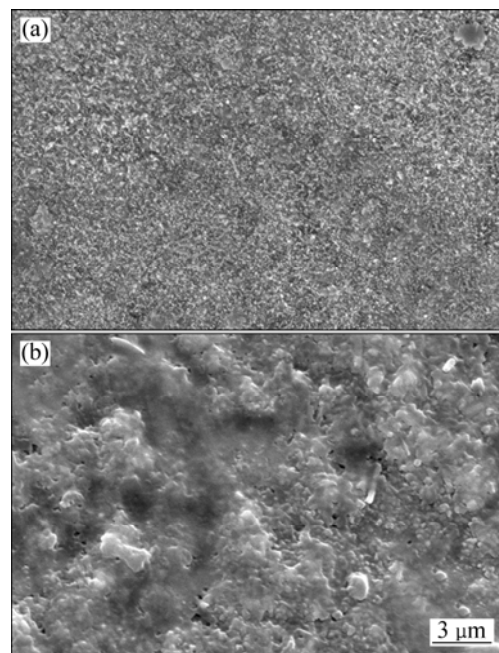


Fig. 5 SEM images showing surface morphologies of oxide scales formed on $(\text{TiB}_2+\text{TiC})/\text{Ni}_3\text{Al}$ composites after 2 h oxidation in air at 900 °C: (a) IC-950; (b) IC-1050

IC-1050. Dense oxidation scale is beneficial for increasing oxidation resistance.

Cross-sectional morphologies of both composites after 50 h oxidation in air at 900 °C are shown in Fig. 6. IC-950 sample formed double sound continuous oxide layers after 50 h exposure. TiO₂ layer with a thickness of around 3 μm is on the top. Al₂O₃ layer with a thickness of around 6 μm is under the TiO₂ layer. Underneath the layers, there is an internal oxidation zone (IOZ) with a thickness of 12 μm. No continuous oxide layer is found on the surface of IC-1050 sample. Oxidized depth of the IC-1050 sample is around 27.5 μm, which is much thicker than the oxidation layer on IC-950.

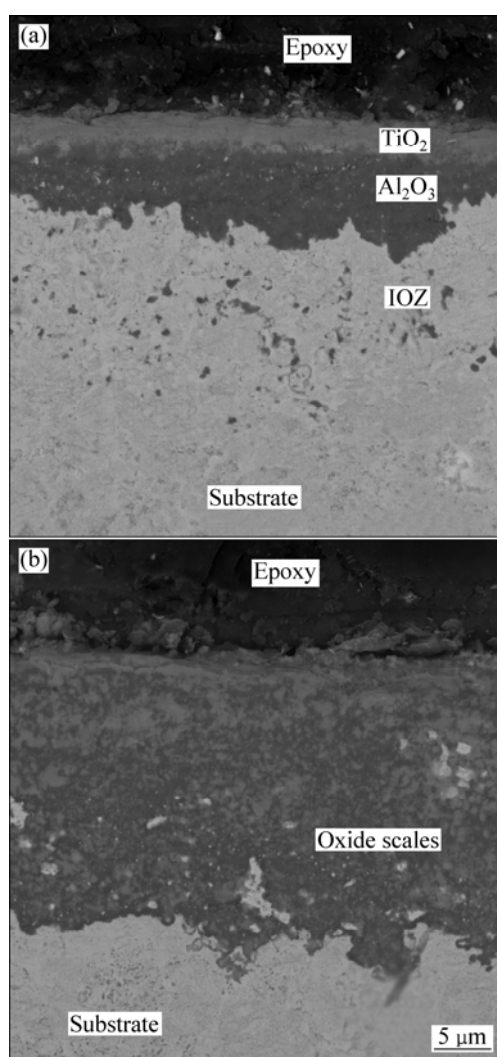


Fig. 6 SEM images showing cross-sectional morphologies of oxide scales formed on (TiB₂+TiC)/Ni₃Al composites after 50 h oxidation in air at 900 °C: (a) IC-950; (b) IC-1050

The XRD (Fig. 7(a)) and EDS results indicate that the oxide scales on IC-950 mainly consist of TiO₂(B) and minor TiO₂ (rutile) after 2 h oxidation, while the oxide scales on IC-1050 is in reverse. TiO₂(B) is a polymorph of TiO₂. The crystal structure of TiO₂(B) is

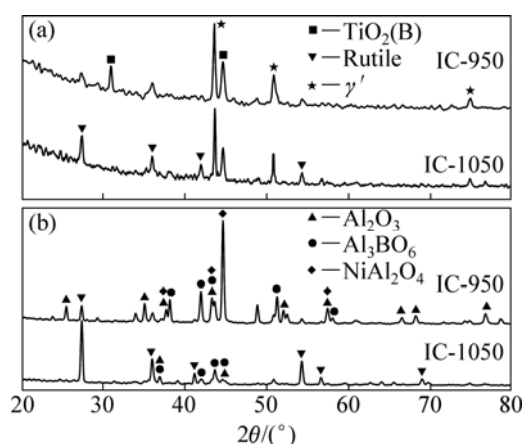


Fig. 7 XRD patterns of (TiB₂+TiC)/Ni₃Al composites cyclic oxidized at 900 °C for 2 h (a) and 50 h (b)

basically the same as that of VO₂(B) [13,14].

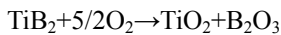
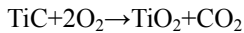
TiO₂(B) is a metastable polymorph [13]. However, our results indicate that this phase can be present at 900 °C. Previous works [15,16] reported that when particle size decreases to sufficiently low value, the total free energy of rutile becomes higher. They also suggested that the number of potential nucleation sites is the rate-limiting factor to rutile formation. These hypotheses suggest that the TiO₂(B) were formed and stable in this work owing to their surface or interfacial energy [17]. Meanwhile, the finer microstructure in IC-950 can provide more nucleation sites due to their smaller size of ceramic particles and great density of grain boundaries, which indicates that the ratio of TiO₂(B) transformation to rutile is smaller in IC-950 than in IC-1050. As a result, there is more TiO₂(B) formed which is more stable in IC-950 than in IC-1050. Experiments to determine the precise relation between the formation of TiO₂(B) and oxidation conditions are in progress.

For the oxide scales formed on IC-950 after 50 h exposure, the XRD (Fig. 7 (b)) and EDS results indicate that the outer oxide layer mainly consists of TiO₂(B) and the inner oxide layer mainly consists of Al₂O₃. In IOZ, Al₂O₃ was formed due to the selective oxidation of Al between the oxide layers and the substrate. The oxide scales formed on IC-1050 consist of major TiO₂(rutile) and a small amount of Al₃BO₆ and NiAl₂O₄. The discontinuous oxide mixtures cannot effectively protect the substrate from the inward diffusion of oxygen [18].

With a similar volume fraction of ceramic particles, IC-950 rather than IC-1050 can form continuous oxide scales. This is related to the different microstructure of the composites, which can be summarized as follows: 1) the spacing between ceramic particles is much smaller in IC-950 than in IC-1050; 2) the grain size of ceramic phases in IC-950 is finer than that in IC-1050; 3) the grain size of Ni₃Al in IC-950 is finer than that in IC-1050.

With these characteristics, IC-950 exhibits an increased ability to grow TiO₂(B) and alumina for the following reasons.

Both TiC and TiB₂ will be oxidized at the tested temperature obeying the following equations [19]:



At the onset of oxidation, ceramic particles in both composites nucleate TiO₂. Taking into account that distribution of ceramic particles in the Ni₃Al matrix was homogeneous, and supposing that the unit cell for the space distribution of ceramic particles in Ni₃Al matrix has a simple cubic structure, the spacing between the initially formed TiO₂ nuclei (d) can be roughly expressed by:

$$d = \left(\sqrt[3]{\frac{4\pi}{3V}} - 2 \right) r$$

where r is the average radius of the ceramic particles and V is the volume fraction of ceramic particles. The calculated d was 30 nm for IC-950 and 225 nm for IC-1050, which means that the spacing between TiO₂ nuclei in IC-950 is dramatically reduced compared with IC-1050. This can also be clearly seen in Fig. 3. As a result, TiO₂ formed on IC-950 is finer than that on IC-1050. As mentioned previously, the more TiO₂ nuclei could stabilize the TiO₂(B) phase. Consequently, there is more TiO₂(B) in the oxide scales formed on IC-950 due to its finer microstructure than that on IC-1050. Meanwhile, the density of TiO₂(B) (3.64 g/cm³) is lower than that of rutile (4.13 g/cm³) [13]. This indicates that it is easier for TiO₂(B) to cover the composite surface due to its larger volume than rutile. As a result, it is easier for IC-950 to form a dense and continuous TiO₂(B) layer than IC-1050 (Fig. 6). The growth of TiO₂(B) on IC-950 can perturb the reaction rate by acting as a gaseous diffusion barrier. Reversely, pores can be clearly seen on the surface of IC-1050 after 2 h oxidation, as shown in Fig. 5. This indicates that rutile as major phase formed on IC-1050 cannot effectively cover the composite surface. And the pores act as quick channel for oxygen diffusion and in turn decrease the oxidation resistance of IC-1050.

Furthermore, Ni₃Al is finer-grained in IC-950 and abundant GBs would enhance Al diffusion to the oxidation front and consequently promote the lateral growth of alumina [6–8]. Once a continuous Al₂O₃ layer formed, the growth of TiO₂ and NiO was obstructed. In contrast, during the oxidation of IC-1050, broad spacing between alumina nuclei makes it impossible for them to form a continuous layer. Ni-rich phase, bright area in Fig. 6, was obviously seen in the oxide scales on

IC-1050. As a result, the microstructure has a great influence on the oxidation performance of the (TiB₂+TiC)/Ni₃Al composites.

4 Conclusions

1) The (TiB₂+TiC)/Ni₃Al composite sintered at 950 °C has a finer microstructure than that sintered at 1050 °C.

2) The microstructure of the (TiB₂+TiC)/Ni₃Al composites has a great impact on oxidation. Finer microstructure could improve the oxidation resistance of the composite.

3) The finely dispersed ceramic particles (TiB₂ and TiC) can promote the formation of compact and continuous TiO₂ oxide layer. Meanwhile, the formation of continuous Al₂O₃ layer between TiO₂ layer and substrate is favored by the ultra-fine-grained Ni₃Al. In contrast, the larger-grained structure of IC-1050 prevents the formation of continuous oxide layer during oxidation.

References

- [1] SHENG L Y, ZHANG W, GUO J T, WANG Z S, OVCHARENKO V E, ZHOU L Z, YE H Q. Microstructure and mechanical properties of Ni₃Al fabricated by thermal explosion and hot extrusion. [J] *Intermetallics*, 2009, 17: 572–577.
- [2] SIKKA V K, DEEVI S C, VISWANATHAN S, SWINDEMAN R W, SANTELLA M L. Advances in processing of Ni₃Al-based intermetallics and applications [J]. *Intermetallics*, 2000, 8: 1329–1337.
- [3] WARDCLOSE C M, MINOR R, DOORBA P J. Intermetallic-matrix composites—A review [J]. *Intermetallics*, 1996, 4: 217–229.
- [4] HE B L, ZHU Y F. Microstructure and properties of TiC/Ni₃Al composites prepared by pressureless melt infiltration with porous TiC/Ni₃Al preforms [J]. *Materials and Manufacturing Processes*, 2011, 26: 586–591.
- [5] QIN F, ANDEREGG J W, JENKS C J, GLEESON B, SORDELET D J, THIE P A. X-ray photoelectron spectroscopy studies of the early-stage oxidation behavior of (Pt, Ni)₃Al(111) surfaces in air. [J] *Surface Science*, 2008, 602: 205–215.
- [6] LIU W, NAKA M. In situ joining of dissimilar nanocrystalline materials by spark plasma sintering [J]. *Scripta Materialia* 2003, 48: 1225–1230.
- [7] CHOUDRY M S, DOLLAR M, EASTMAN J A. Nanocrystalline NiAl—Processing, characterization and mechanical properties [J]. *Materials Science and Engineering A*, 1998, 256: 25–33.
- [8] SHEARWOOD C, FU Y Q, YU L, KHOR K A. Spark plasma sintering of TiNi nano-powder [J]. *Scripta Materialia*, 2005, 52: 455–460.
- [9] BECHER P F, PLUCKNETT K P. Properties of Ni₃Al-bonded titanium carbide ceramics [J]. *Journal of European Ceramic Society*. 1997, 18: 395–400.
- [10] BANFIELD J F, VEBLEN D R, SMITH D J. The identification of naturally occurring TiO₂ (B) by structure determination using high-resolution electron microscopy, image simulation, and distance-least-squares refinement [J]. *American Mineralogist*, 1991, 76: 343–353.
- [11] BANFIELD J F, VEBLEN D R. Conversion of perovskite to anatase

- and TiO₂ (B): A TEM study and the use of fundamental building blocks for understanding relationships among the TiO₂ minerals [J]. American Mineralogist, 1992, 77: 545–557.
- [12] ZHANG H, BANFIELD J F. Thermodynamic analysis of phase stability of nanocrystalline titania [J]. J Mater Chem, 1998, 8: 2073–2076.
- [13] GRIBB A A, BANFIELD J F. Particle size effects on transformation kinetics and phase stability in nanocrystalline TiO₂ [J]. American Mineralogist, 1997, 82: 717–728.
- [14] KOGURE T, UMEZAWA T, KOTANI Y, MATSUDA A, TATSUMISAGO M, MINAMI T. Formation of TiO₂(B) nanocrystallites in sol-gel-derived SiO₂-TiO₂ film [J]. J Am Ceram Soc, 1999, 82: 3248–3250.
- [15] BAI C Y, LUO Y J, KOO C H. Improvement of high temperature oxidation and corrosion resistance of superalloy IN-738LC by pack cementation [J]. Surface and Coatings Technology, 2004, 183: 74–88.
- [16] RUDOLPH P, BRZEZINKA K W, WÄSCHE R, KAUTEK W. Physical chemistry of the femtosecond and nanosecond laser-material interaction with SiC and a SiC-TiC-TiB₂ composite ceramic compound [J]. Applied Surface Science, 2003, 208–209: 285–291.
- [17] LIU Z Y, GAO W, DAHM K L, WANG F H. Oxidation behaviour of sputter-deposited Ni-Cr-Al micro-crystalline coatings [J]. Acta Mater, 1998, 46: 1691–1700.
- [18] WANG F H. Oxidation resistance of sputtered Ni₃(Al, Cr) nanocrystalline coating [J]. Oxidation of Metals, 1997, 47: 247–258.
- [19] PENG X, LI M, WANG F. A novel ultrafine-grained Ni₃Al with increased cyclic oxidation resistance [J]. Corrosion Science. 2011, 53: 1616–1620.

晶粒尺寸对(TiB₂+TiC)/Ni₃Al 复合材料循环氧化性能的影响

曹国剑¹, 许虹宇², 郑镇洙², 耿林², 奈贺正明³

1. 哈尔滨理工大学 材料科学与工程学院, 哈尔滨 150040;

2. 哈尔滨工业大学 材料科学与工程学院, 哈尔滨 150001;

3. 大阪大学 接合研究所, 日本大阪 567-0047

摘要: 采用放电等离子烧结法制备(TiB₂+TiC)/Ni₃Al 复合材料。在 950 °C 下烧结的(TiB₂+TiC)/Ni₃Al 复合材料的组织比在 1050 °C 下烧结的(TiB₂+TiC)/Ni₃Al 复合材料的组织更细小。对烧结温度分别为 950 °C 和 1050 °C 的复合材料在 900 °C 下进行循环氧化性能测试。结果表明, 在 950 °C 下烧结的复合材料的循环氧化质量损失要小于在 1050 °C 下烧结的复合材料的。晶粒细化有助于在氧化过程汇总的选择性氧化, 使得连续的 TiO₂ 和 Al₂O₃ 氧化膜得以在复合材料表面形成, 从而提高复合材料的抗氧化性能。

关键词: Ni₃Al; 复合材料; 晶粒细化; 氧化; 机械合金化

(Edited by YANG Hua)